RESEARCH ON DYNAMIC CHARACTERISTICS OF A DOUBLE-PENDULUM SUSPENSION FOR A BOOM SPRAYER
/
喷杆喷雾机双摆悬架动力学特性研究

Fang LI[1)], Xiaohu BAI*[2)]
[1)] School of Information and Control Engineering, Liaoning Petrochemical University, Fushun/China;
[2)] College of Engineering, Shenyang Agricultural University, Shenyang/China
E-mail: baixiaohu@syau.edu.cn
DOI: https://doi.org/10.35633/inmateh-71-20

Keywords: *dynamic model, passive suspension, active suspension, transient response, frequency response*

ABSTRACT
During the operation of a boom sprayer, various excitations can cause the boom to roll, yaw, or jolt, which can negatively impact the spray effect. In order to maintain the stability of the boom, it is crucial to incorporate a suspension between the vehicle body and the boom. This study established a dynamic model that describes the roll of a boom mounted on a double-pendulum suspension. The transfer function and frequency response function of the passive suspension were obtained, with the ground slope angle as input and the boom inclination angle as output. The analysis results showed that the passive suspension can partially isolate high-frequency disturbances but cannot follow low-frequency signals. For the active suspension, the transient and frequency responses were analyzed by numerical integration algorithm, the harmonic balance method and numerical solution. The results indicated that the active suspension can enable the boom to follow the ground slope, track low-frequency signals to a certain extent, and isolate high-frequency signals. The proposed mathematical model can be utilized to analyze the dynamic characteristics and provide guidance for the double-pendulum suspension design.

摘要
喷杆喷雾机田间作业时，各种激励会导致喷杆产生翻滚、偏转、振荡运动，对喷雾效果产生不利影响。为了保持喷杆稳定，在车体与喷杆之间安装悬架非常重要。本文建立了描述安装在双摆悬架上的喷杆翻滚运动的动力学模型。针对被动悬架，得出了以地面坡角为输入、喷杆倾角为输出的传递函数及频率响应函数，分析结果表明，被动悬架能在一定程度上隔离高频扰动，但不能跟踪低频信号。针对主动悬架，采用数值积分算法、谐波平衡法和数值解法分析了瞬态响应和频率响应。结果表明，主动悬架能使喷杆跟随地面坡角变化，可以在一定程度上跟踪低频信号，隔离高频信号。建立的数学模型可以用来分析双摆悬架的动力学特性，为喷雾机悬架设计提供参考。

INTRODUCTION

The effectiveness and efficiency of chemical spraying in agriculture is heavily influenced by the quality of plant protection equipment (*He, 2020*). Boom sprayers are commonly utilized due to their wide coverage and high productivity in applying chemical materials such as pesticides, herbicides, and fertilizers (*He, 2022; Qiu et al., 2015*). However, the motion of the boom caused by tractor vibration and uneven terrain can result in uneven distribution of the chemical agents. Rolling, yawing, and jolting are the primary types of motion that affect the boom in the vertical and horizontal planes. These motions will lead to harmful over-application or under-application of chemical agents (*Jeon et al. 2013; Langenakens et al.1999*). Although yawing and jolting have a greater impact on spray consistency, most boom sprayers are equipped with a vertical suspension to mitigate rolling (*Ramon et al., 1997; Cui et al., 2019*). Various types of vertical suspensions have been developed, including pendulum, trapezium, cable, and Douven suspensions (*Deprez et al., 2003*). Double-pendulum suspensions have gained popularity among manufacturers, with the first pendulum serving as a passive suspension and the second pendulum acting as an active suspension (*Tahmasebi et al., 2013*).

Fang Li, Lecturer, Ph.D.; Xiaohu Bai, Associate Prof., Ph.D.,Corresponding Author.

Theoretical investigations have been conducted for certain types of suspensions. O'Sullivan proposed mathematical models for both passive and active versions of a pendulum boom suspension, and simulated their transient and frequency responses (*O'Sullivan, 1986*). Experimental results confirmed the accuracy of the suspension models and demonstrated their usefulness in designing an appropriate pendulum suspension (*O'Sullivan, 1988*). Frost presented a mathematical model for an active twin-link boom suspension and its response to the rolling motion of the spray vehicle (*Frost, 1984*). Deprez et al. studied several suspension models, including a slow active pendulum suspension, a slow active trapezium suspension, a cable suspension, and a suspension based on following a curved profile, and found that they have the same mathematical model structure (*Deprez et al., 2002*). Anthonis et al. developed a parameterized mathematical model for the double pendulum suspension of the 39 m sprayer of John Deere, and optimized the distance to the rotation point of the damper and the appropriate damping value (*Anthonis et al., 2005*). Wu and Miao established a model with four spring-damper modules between the boom and the frame, and investigated the frequency response of the model under different excitation signals (*Wu et al., 2012*). Xue et al. added a hydraulic cylinder to the two-link trapezoidal spray boom passive suspension to obtain an active suspension, and simulated and analyzed its dynamic characteristics for controller design by MATLAB/SIMULINK (*Xue et al., 2018*). Cui et al. established a nonlinear dynamic model and geometric equation of the pendulum active and passive suspension system to design an adaptive robust controller (*Cui et al., 2020*). Zhuang designed a suspension with the combination of springs and dampers, and analyzed the dynamic and kinematic vibration characteristics of the boom by modal simulation and field tests (*Zhuang, 2020*). *Zhang, (2021),* designed an active and passive suspension based on the pendulum and isosceles trapezoid principle, established the dynamic model of the boom, and simulated the instantaneous response and frequency response by ADAMS vibration simulation technology. Yan et al. developed a geometric continuous model of spray boom vibration considering the influence of the boom sprayer body and boom suspension, and studied the dynamic behavior of the spray boom under step excitation (*Yan, 2021*). However, little research has been devoted to the effects of springs and dampers on the dynamic behavior of the double-pendulum suspension.

This paper presents a mathematical model for the double-pendulum suspension, which takes into account the influence of springs and dampers. The response of the boom is analyzed in both time and frequency domains for both passive and active suspensions. The aim of this study is to provide references for the design and parameter setting of the boom suspension.

MATERIALS AND METHODS

Structure and principle of the double-pendulum suspension

The double-pendulum suspension is comprised of two pendulum rods, height sensors, springs, dampers, and an actuator, as illustrated in Figure 1. The first pendulum rod is articulated to the frame and the second pendulum rod at O_1 and O_2, respectively. The boom is rigidly fixed to the second pendulum rod at G, the gravity center of the boom. A spring and a damper are connected between the first pendulum rod and the frame attached to the vehicle. An actuator is installed between the first and second pendulum rod.

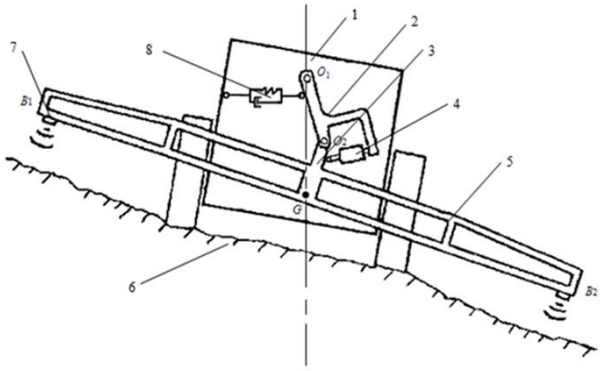

Fig. 1 - Structure of the double-pendulum suspension

1– frame; 2- first pendulum rod; 3- second pendulum rod; 4- actuator; 5- boom; 6- ground; 7- height sensor; 8- spring and damper

In the event that the power supply is deactivated and the actuator length remains constant, the suspension becomes passive, causing the boom to pivot only around O_1. A special case arises when the angle between the first and second pendulum rods is zero, indicating that the boom's balance position is horizontal, with its gravity center G below the hinge point O_1.

However, if the actuator length is either increased or decreased, the boom's gravity center will shift to the left or right, respectively, resulting in a non-horizontal equilibrium position. Consequently, by continuously regulating the actuator length, the suspension becomes active, enabling the boom to adapt to variations in ground slope.

Modelling of the Double-Pendulum Suspension

Passive Suspension

The suspension's parameters are presented in Figure 2.

Fig. 2 - Parameters of the double-pendulum suspension

The angles α, β, and γ represent the inclination of the ground to the horizontal, the inclination of the first pendulum rod to the vertical, and the inclination of the boom to the horizontal, respectively. The angle θ denotes the angle between the first and second pendulum rods. When θ remains constant at zero, the suspension becomes passive. For the generalized coordinate β, by applying the second Lagrange equation, the equation of the boom motion can be derived as:

$$\frac{d}{dt}\left(\frac{\partial E_k}{\partial \dot{\beta}}\right)-\frac{\partial E_k}{\partial \beta}=Q_\beta-\frac{\partial \psi}{\partial \dot{\beta}} \tag{1}$$

where, E_k represents the kinetic energy of the boom, N·m; Q_β represents the generalized force, N; ψ represents the dissipation function, N·m·rad/s.

The kinetic energy of the boom can be expressed as:

$$E_k=\frac{1}{2}I\dot{\beta}^2+\frac{1}{2}m\left[l_4{}^2\dot{\alpha}^2+(l_1+l_2)^2\dot{\beta}^2-2l_4(l_1+l_2)\dot{\alpha}\dot{\beta}\cos(\alpha-\beta)\right] \tag{2}$$

where, I represents the moment of inertia of the boom about the axis through G, kg·m^2; m represents the mass of the boom, kg; l_1 represents the length of the first pendulum, m; l_2 represents the length of the second pendulum, m; l_4 represents the distance between O_1 and the ground, m.

The generalized force can be expressed as:

$$Q_\beta=-mg(l_1+l_2)\sin\beta+k(\alpha-\beta)l_s{}^2 \tag{3}$$

where, k represents the stiffness coefficient of the spring, N/m; l_s represents the distance from the spring's installation position to O_1, m.

The dissipation function can be expressed as:

$$\psi=\frac{1}{2}c[l_d(\dot{\alpha}-\dot{\beta})]^2 \tag{4}$$

Where, c represents the damping coefficient of the damper, N·s/m; l_d represents the distance from the damper's installation position to O_1, m.

Assuming that α and β are small, ignoring the second-order terms, and substituting equations (2), (3) and (4) into equation (1), the equation of the boom motion can be stated in the following form.

$$\ddot{\beta}[I+m(l_1+l_2)^2]+\dot{\beta}cl_d^{\ 2}+\beta[mg(l_1+l_2)+kl_s^{\ 2}]=\ddot{\alpha}ml_4(l_1+l_2)+\dot{\alpha}cl_d^{\ 2}+\alpha kl_s^{\ 2} \quad (5)$$

When the angle θ is equal to zero, the angle γ is equal to the angle β. Therefore, by performing the Laplace transform on equation (5) and rearranging the terms, the transfer function linking the inclination angle of the boom, γ, to the inclination angle of the ground, α, can be derived as:

$$H(s)=\frac{ml_4(l_1+l_2)s^2+cl_d^{\ 2}s+kl_s^{\ 2}}{[I+m(l_1+l_2)^2]s^2+cl_d^{\ 2}s+mg(l_1+l_2)+kl_s^{\ 2}} \quad (6)$$

Substituting $j\omega$ for s in equation (6), the frequency response function can be achieved as:

$$H(j\omega)=\frac{-ml_4(l_1+l_2)\omega^2+jcl_d^{\ 2}\omega+kl_s^{\ 2}}{-[I+m(l_1+l_2)^2]\omega^2+jcl_d^{\ 2}\omega+mg(l_1+l_2)+kl_s^{\ 2}} \quad (7)$$

Active Suspension

When the sprayer travels over undulating terrain, the actuator should be adjusted by extending or retracting it in order to maintain the boom parallel to the ground. This ensures that the suspension remains active. For the generalized coordinates β and γ, by applying the Lagrange equation of the second kind, the equations of the boom motion can be expressed as:

$$\frac{d}{dt}\left(\frac{\partial E_k}{\partial\dot{\beta}}\right)-\frac{\partial E_k}{\partial\beta}=Q_\beta-\frac{\partial\psi}{\partial\dot{\beta}} \quad (8)$$

$$\frac{d}{dt}\left(\frac{\partial E_k}{\partial\dot{\gamma}}\right)-\frac{\partial E_k}{\partial\gamma}=Q_\gamma-\frac{\partial\psi}{\partial\dot{\gamma}} \quad (9)$$

The kinetic energy of the boom can be expressed as:

$$E_k=\frac{1}{2}I\dot{\gamma}^2+\frac{1}{2}m\left[\dot{\alpha}^2l_4^{\ 2}+\dot{\beta}^2l_1^{\ 2}+\dot{\gamma}^2l_2^{\ 2}-2\dot{\alpha}\dot{\beta}l_1l_4-2\dot{\alpha}\dot{\gamma}l_2l_4+2\dot{\beta}\dot{\gamma}l_1l_2\right] \quad (10)$$

The generalized force can be expressed as:

$$Q_\beta=-(mgl_1+kl_s^{\ 2})\beta+kl_s^{\ 2}\alpha-Fl_3 \quad (11)$$

$$Q_\gamma=-mgl_2\gamma+Fl_3 \quad (12)$$

where, F represents the force exerted by the actuator, N; l_3 represents the distance between the installation position of the actuator and the point O_2, m.

Substituting equations (4), (10), and (11) into equation (8), and equations (4), (10), and (12) into equation (9), the equations of the boom motion can be stated in the following form.

$$-ml_1l_4\ddot{\alpha}+ml_1^{\ 2}\ddot{\beta}+ml_1l_2\ddot{\gamma}+cl_d^{\ 2}(\dot{\beta}-\dot{\alpha})+(mgl_1+kl_s^{\ 2})\beta-\alpha kl_s^{\ 2}=-Fl_3 \quad (13)$$

$$(I+ml_2^{\ 2})\ddot{\gamma}-ml_2l_4\ddot{\alpha}+ml_1l_2\ddot{\beta}+mgl_2\gamma=Fl_3 \quad (14)$$

In order to enable the boom to follow ground undulations, the active suspension employs proportional control. This entails that the actuator velocity is directly proportional to the difference between the ground angle α and the boom inclination angle γ. The time delay caused by the sensor, signal processor, and actuator can be represented by an inertia loop. Therefore, the transfer function relating the actuator velocity to the difference between α and γ can be expressed as:

$$\frac{V(s)}{A(s)-R(s)}=\frac{K_p}{Ts+1} \quad (15)$$

Where,

$V(s)$, $A(s)$, and $R(s)$ represent the image functions of the actuator velocity v, the ground angle α, and the boom inclination angle γ in the frequency domain, respectively; K_p is the proportional coefficient of the inertia loop, $ms^{-1}rad^{-1}$; T is the time constant of the inertia loop, s.

The relationship between the velocity of the actuator and its displacement can be expressed mathematically as:

$$V(s)=sD(s) \quad (16)$$

From equations (15) and (16), the transfer function between *d* and (*α*-*γ*) can be derived as:

$$\frac{D(s)}{A(s)-R(s)}=\frac{K_p}{(Ts+1)s} \tag{17}$$

Through the application of inverse Laplace transformation, equation (17) can be changed to

$$T\ddot{d}+\dot{d}=K_p(\alpha-\gamma) \tag{18}$$

When *θ* is very small, the actuator displacement *d* is given by

$$d=l_3\theta=l_3(\gamma-\beta) \tag{19}$$

Substituting equation (19) into equation (18), the following equation can be obtained.

$$Tl_3\ddot{\gamma}-Tl_3\ddot{\beta}+l_3\dot{\gamma}-l_3\dot{\beta}-K_p\alpha+K_p\gamma=0 \tag{20}$$

The group of differential equations comprising equations (13), (14), and (20) describes the dynamic characteristics of the boom. If the ground angle *α* is known, the boom inclination angle and the actuator output can be calculated.

Assuming a step signal for the ground angle *α*, and defining the state variables, namely $x_1=\beta$, $x_2=\dot{\beta}$, $x_3=\gamma$, and $x_4=\dot{\gamma}$, the solution to equations (13), (14), and (20) can be converted into state equations as:

$$\begin{cases}\dot{x}_1=x_2\\ \dot{x}_2=\dfrac{1}{a+b}[\dfrac{b}{T}x_4-(\dfrac{b}{T}+cl_d{}^2)x_2+(\dfrac{K_pb}{Tl_3}-mgl_2)x_3-(mgl_1+kl_s{}^2)x_1+(kl_s{}^2-\dfrac{K_pb}{Tl_3})\alpha]\\ \dot{x}_3=x_4\\ \dot{x}_2=\dfrac{1}{a+b}[-\dfrac{a}{T}x_4+(\dfrac{a}{T}-cl_d{}^2)x_2-(\dfrac{K_pa}{Tl_3}+mgl_2)x_3-(mgl_1+kl_s{}^2)x_1+(kl_s{}^2+\dfrac{K_pa}{Tl_3})\alpha]\end{cases} \tag{21}$$

According to equation (21), the boom angle *γ* can be calculated by using the Runge-Kutta numerical integration algorithm and calling the ode45 function in MATLAB.

From equations (13), (14), and (20), it is difficult to obtain the frequency response function of the suspension with the ground angle α as the input and the boom angle γ as the output. Therefore, the harmonic balance method and numerical solution were adopted to calculate the frequency response (*Geng et al., 2013; Bai et al., 2000*).

Considering the first harmonic balance, $\alpha=\mathrm{A}_\alpha\sin(\omega t)$, $\beta=\mathrm{A}_\beta\sin(\omega t+\varphi_\beta)$, and $\gamma=\mathrm{A}_\gamma\sin(\omega t+\varphi_\gamma)$ can be set. Subsequently, the following nonlinear equations can be derived from equations (13), (14), and (20).

$$(mgl_2-b\omega^2)A_\gamma+(mgl_1+K-a\omega^2)A_\beta\cos(\varphi_\beta-\varphi_\gamma)-C\omega A_\beta\sin(\varphi_\beta-\varphi_\gamma)+[m(l_1+l_2)l_4\omega^2-K]A_\alpha\cos\varphi_\gamma-CA_\alpha\omega\sin\varphi_\gamma=0 \tag{22}$$

$$(mgl_1+K-a\omega^2)A_\beta\sin(\varphi_\beta-\varphi_\gamma)+C\omega A_\beta\cos(\varphi_\beta-\varphi_\gamma)-[m(l_1+l_2)l_4\omega^2-K]A_\alpha\sin\varphi_\gamma-CA_\alpha\omega\cos\varphi_\gamma=0 \tag{23}$$

$$Tl_3A_\beta\omega^2+(K-Tl_3\omega^2)A_\gamma\cos(\varphi_\gamma-\varphi_\beta)-l_3A_\gamma\omega\sin(\varphi_\gamma-\varphi_\beta)-K_pA_\alpha\cos\varphi_\beta=0 \tag{24}$$

$$-l_3A_\beta\omega+(K-Tl_3\omega^2)A_\gamma\sin(\varphi_\gamma-\varphi_\beta)+l_3A_\gamma\omega\cos(\varphi_\gamma-\varphi_\beta)+K_pA_\alpha\sin\varphi_\beta=0 \tag{25}$$

Equations (22), (23), (24), and (25) demonstrate the frequency response of the suspension. By solving these equations, the amplitude-frequency response of the active suspension can be determined, given a certain value for A_α.

RESULTS

Characteristics of Passive Suspension in Time Domain

When a sprayer works in a farm, the ground angle *α* may suddenly change due to the uneven terrain, which can be represented by a step signal (*Cui et al., 2019*). According to equation (6), the unit step response curves of the suspension can be acquired.

The suspension rotational damping coefficient is expressed as $C=cl_d^2$, while the suspension rotational stiffness coefficient is denoted as $K=kl_s^2$ (*Cui et al., 2017a*, *Cui et al., 2017b*). The parameters of the suspension were set as follows: m=67kg, I=110kg·m^2, l_1=0.45m, l_2=0.25m, l_4=0.96m (*O'Sullivan, 1988*).

When the value of K is equal to zero, the unit step response curves of the suspension with varying rotational damping coefficients are depicted in Figure 3.

When subjected to a unit step signal, the boom inclination angle initially rises from its starting point, subsequently decreases rapidly, and gradually returns to its state of equilibrium. The initial value of the boom inclination angle is irrelevant to the damper. Raising the rotational damping coefficient leads to a reduction in overshooting and settling time, as well as an increase in response speed. This is advantageous for quickly bringing the boom back to its stable state. However, as the rotational damping coefficient increases, the maximum value of the boom inclination angle also increases. This can result in the boom end coming into contact with either the crop or the ground.

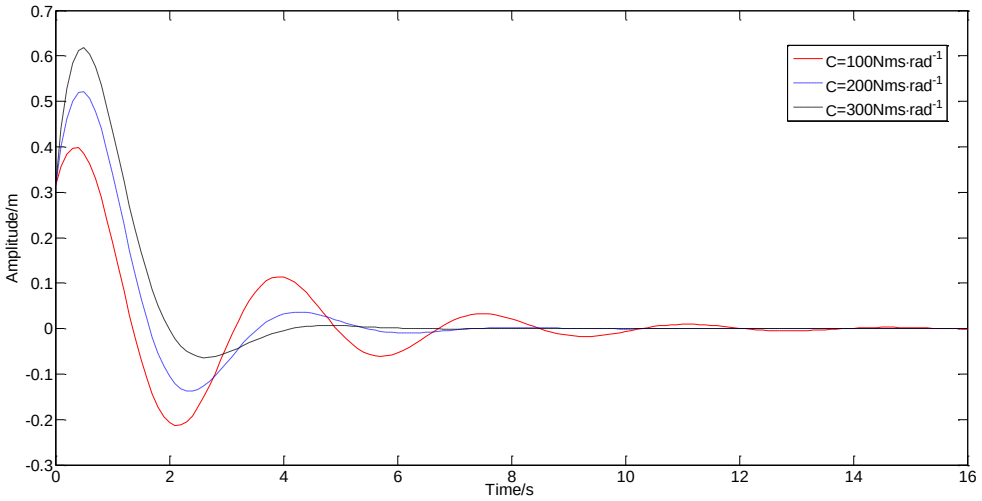

Fig. 3 - Unit step response curves with varying rotational damping coefficients

With C assigned a value of 300 Nms·rad^{-1}, the unit step response curves of the suspension with varying rotational stiffness coefficients are depicted in Figure 4.

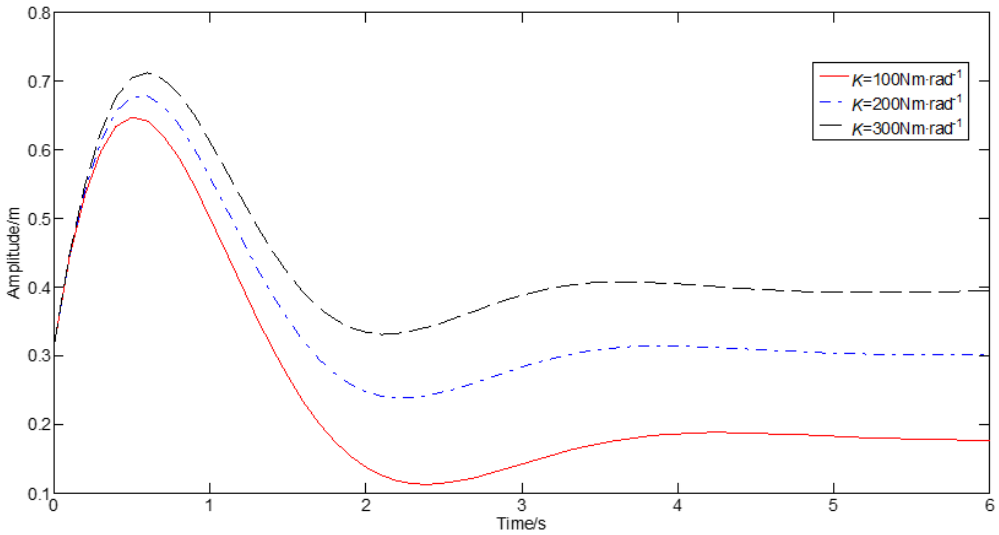

Fig. 4 - Unit step response curves with varying rotational stiffness coefficients

Characteristics of Passive Suspension in Frequency Domain

According to equation (7), the amplitude-frequency characteristic curves of the suspension can be acquired. When the value of K is equal to zero, the amplitude-frequency characteristic curves of the suspension with varying rotational damping coefficients are depicted in Figure 5.

The amplitude ratio of the boom angle *γ* to the ground angle *α* displays an initial increase in response to an increase in frequency, reaching its maximum value, and subsequently decreasing until it stabilizes at a constant value. When the excitation frequency matches the resonant frequency of the suspension, the amplitude ratio reaches its maximum value. The resonant frequency remains unaffected by the rotational damping coefficient. At this particular frequency, the amplitude ratio experiences a decline as the rotational damping coefficient increases. This suggests that an increase in damping can effectively mitigate the resonance between the suspension and the ground. Nevertheless, as damping increases, the suspension's ability to attenuate high-frequency excitation slows down.

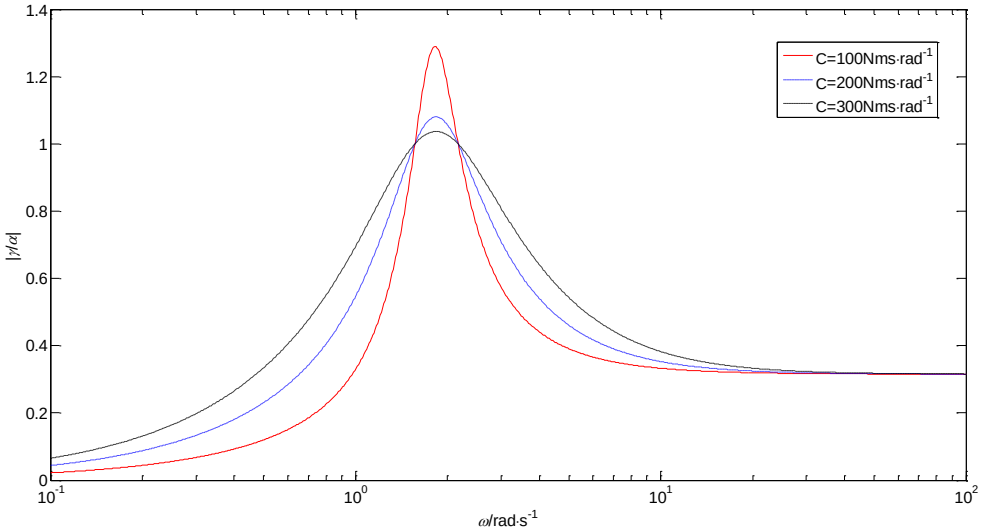

Fig. 5 - Amplitude-frequency characteristic curves with varying rotational damping coefficients

With *C* assigned a value of 300 Nms·rad^{-1}, the amplitude-frequency characteristic curves of the suspension with varying rotational stiffness coefficients are depicted in Figure 6.

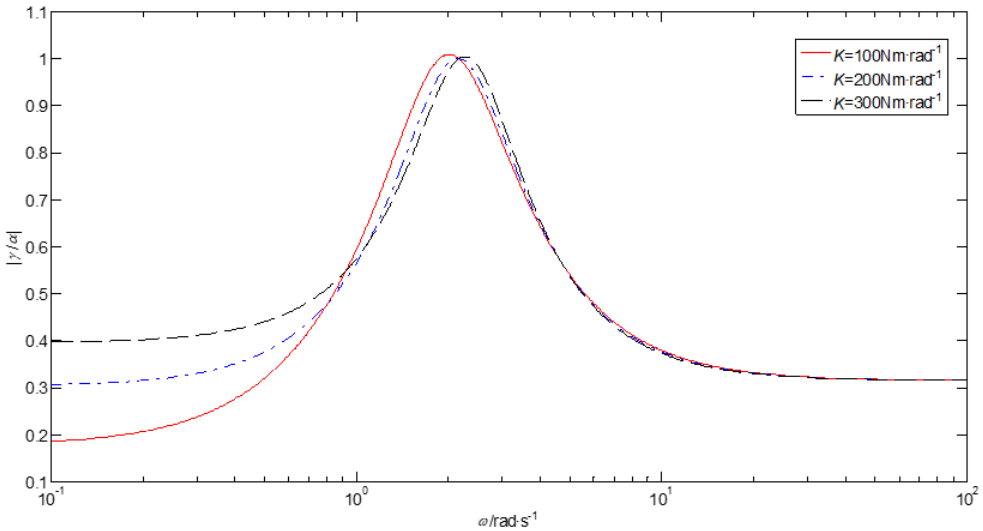

Fig. 6 - Amplitude-frequency characteristic curves with varying rotational stiffness coefficients

As the rotational stiffness coefficient increases, the resonant frequency also increases. This causes the ground disturbance to be easily transmitted to the boom across a wider frequency range. Consequently, the stability of the boom is compromised. At lower frequencies, an increase in the rotational stiffness coefficient leads to a rise in the amplitude ratio, which gradually approaches 1. This implies that an increase in the rotational stiffness coefficient is advantageous in making the boom follow the ground. The amplitude ratio of higher frequencies remains largely unaffected by an increase in the rotational stiffness coefficient.

Characteristics of Active Suspension in Time Domain

The ground angle α was established at 0.3 rad, considering the actual condition of hilly areas (*Cui et al., 2017a*; *Cui et al., 2017b*). The parameters for the boom were determined as m=67 kg, I=110 kg·m^2. Under the given conditions of l_1=0.45 m, l_2=0.25 m, l_3=0.2 m, K_p=0.3 ms^{-1}rad^{-1}, T=0.1 s, and K=0, the effect of rotational damping coefficients on the boom angle is demonstrated in Figure 7.

As the rotational damping coefficient of the suspension decreases, there is an increase in overshoot and settling time, resulting in a decline in stability. However, the response speed remains relatively unchanged. When utilizing the suspension parameters mentioned above and C is less than 90 Nms·rad^{-1}, the system will fail to converge and the boom will be unable to work normally.

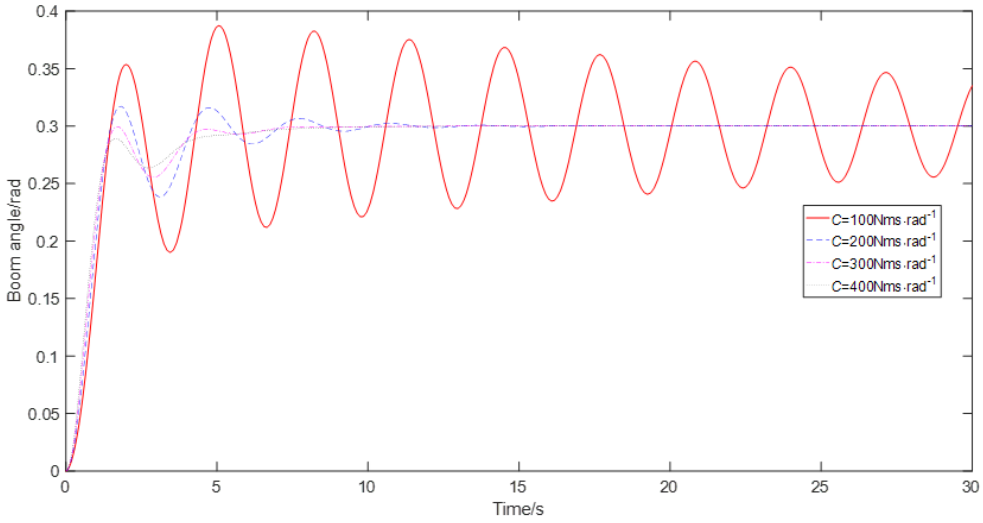

Fig. 7 - Effect of rotational damping coefficients on the boom angle

Under the given conditions of l_1=0.45 m, l_2=0.25 m, l_3=0.2 m, K_p=0.1 ms^{-1}rad^{-1}, T=0.1 s, and C=100 Nms·rad^{-1}, the effect of rotational stiffness coefficients on the boom angle is demonstrated in Figure 8.

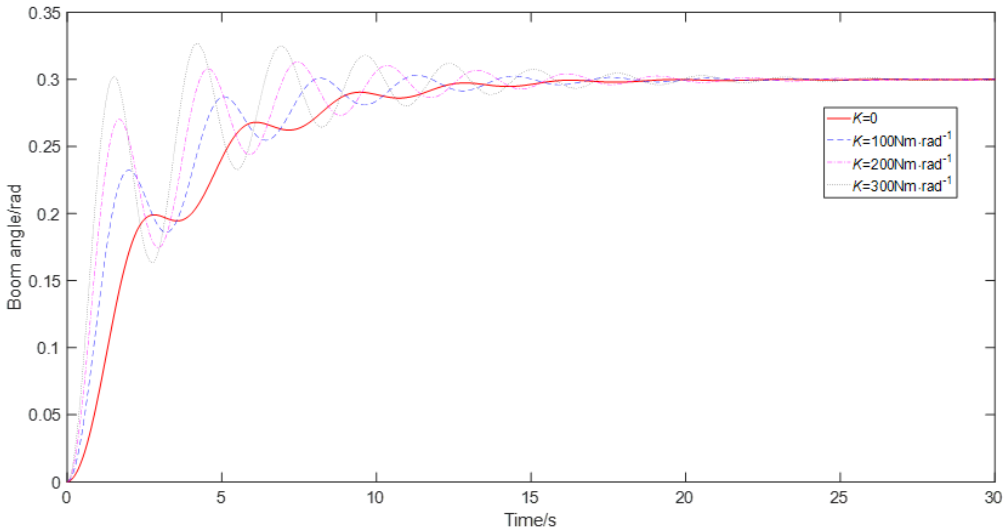

Fig. 8 - Effect of rotational stiffness coefficients on the boom angle

As the rotational stiffness coefficient of the suspension increases, the system exhibits a faster response and an increase in overshoot and settling time. In order to make the boom follow ground undulations quickly, the incorporation of springs through active suspensions can be effective. It is important to note, however, that the K value should not be excessively high as this may result in a prolonged settling time. Furthermore, if the proportional coefficient is large, an excessive K value may lead to system instability and hinder the proper functioning of the boom.

Characteristics of Active Suspension in Frequency Domain

The amplitude of the ground angle α was established at 0.3 rad. The parameters for the boom were determined as m=67 kg, I=110 kg·m^2. Under the given conditions of l_1=0.45 m, l_2=0.25 m, l_3=0.2 m, l_4=0.9 m, K_p=1 ms^{-1}rad^{-1}, C=100 Nms·rad^{-1}, T=0.1 s, and K=0, the amplitude-frequency response of the active suspension is shown in Figure 9.

At low excitation frequencies, specifically between point A and point B on the curve, the amplitude ratio of the boom angle γ to the ground angle α is approximately 1, which is a desirable outcome. The amplitude ratio experiences a slight decrease as it progresses from point B to point C, followed by a gradual increase from point C to point D. The maximum amplitude ratio is observed at point D, which corresponds to the resonant frequency of the active suspension. When the excitation frequency is greater than the resonant frequency, a swift decline in the amplitude ratio is observed, eventually stabilizing at a constant value. This phenomenon is similar to the frequency response of the passive suspension. As a result, a well-designed active suspension has the capability to effectively track low-frequency signals while attenuating high-frequency signals.

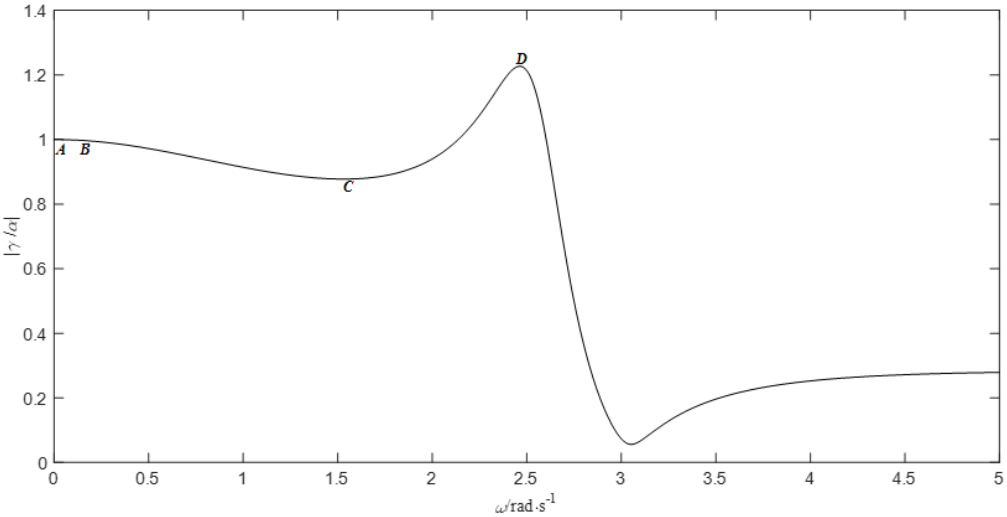

Fig. 9 - Amplitude-frequency response of the active suspension

CONCLUSIONS

The present study established a dynamic model that characterizes the roll of a spray boom equipped with a double-pendulum suspension, utilizing the second Lagrange equation. The transfer function and frequency response function of the passive suspension were derived with the ground slope angle as input and the boom inclination angle as output. The analysis results indicate that the passive suspension can partially attenuate high-frequency disturbances, but is unable to track low-frequency signals. Furthermore, the amplitude ratio of the boom inclination angle to the ground slope angle approaches a stable value beyond the resonant frequency as the frequency increases.

The transient response of the active suspension was analyzed through the utilization of a numerical integration algorithm. The frequency response was calculated using the harmonic balance method and numerical solution. The findings suggest that the active suspension, when equipped with suitable configuration and control parameters, can facilitate the boom's ability to track variations in the ground slope angle. At low frequencies, the amplitude ratio is approximately 1, but it declines sharply beyond the resonant frequency. This implies that the active suspension can effectively track low-frequency signals while partially isolating high-frequency signals.

The mathematical model presented in this paper has the potential to facilitate an analysis of the dynamic characteristics of the spray boom, thereby offering valuable insights for the design of its suspension.

ACKNOWLEDGEMENTS

This research was supported by talent scientific research fund of Liaoning Petrochemical University（No.2021XJJL-024）.

REFERENCES

[1] Anthonis, J., Audenaert, J., Ramon, H. (2005). Design optimization for the vertical suspension of a crop sprayer boom. *Biosystems Engineering*, 90(2), 153–160.

[2] Bai, H., Zhang, P., Huang, X. (2000). Study on the response computation method of a two degrees-of-freedom vibration absorber system with variable coefficient of sliding friction using optimum approximate technique (干摩擦动力吸振器简谐激励响应计算的最优化方法研究). *Journal of Vibration Shock*, 19(3), 43–46.

[3] Cui, L., Xue, X., Ding, S., Qiao, B., Le, F. (2017a). Analysis and test of dynamic characteristics of large spraying boom and pendulum suspension damping system (大型喷杆及其摆式悬架减振系统动力学特性分析与试验). *Transactions of the Chinese Society of Agricultural Engineering*, 33(9), 69–76.

[4] Cui, L., Xue, X., Ding, S., Gu, W., Chen, C, Le, F. (2017b). Modeling and simulation of dynamic behavior of large spray boom with active and passive pendulum suspension (双钟摆主被动悬架式大型喷雾机喷杆动力学仿真与试验). *Transactions of the Chinese Society of Agricultural Machinery*, 48(2), 82–90.

[5] Cui, L., Xue, X., Le, F., Mao, H., Ding, S. (2019). Design and experiment of electro hydraulic active suspension for controlling the rolling motion of spray boom. International *Journal of Agricultural and Biological Engineering*, 12(4), 72–81.

[6] Cui, L., Xue, X., Le, F., Ding, S. (2019). Design and evaluation method of testing bench for spray boom suspension systems (大型喷杆悬架系统测试平台设计与评价方法研究). *Transactions of the Chinese Society of Agricultural Engineering*, 35(16), 23–31.

[7] Cui, L., Xue, X., Le, F., Ding, S. (2020). Adaptive robust control of active and passive pendulum suspension for large boom sprayer (大型喷杆喷雾机钟摆式主被动悬架自适应鲁棒控制研究). *Transactions of the Chinese Society of Agricultural Machinery*, 51(12), 130–141.

[8] Deprez, K., Anthonis, J., Ramon, H. (2002). Development of a slow active suspension for stabilizing the roll of spray booms: part 1-Hybrid modelling. *Biosystems Engineering*, 81(2), 185–191.

[9] Deprez, K., Anthonis, J., Ramon, H. (2003). System for vertical boom corrections on hilly fields. *Journal of Sound Vibration*, 266(3), 613–624.

[10] Frost, A.R. (1984). Simulation of an active spray boom suspension. *Journal of Agricultural Engineering Research*, 30, 313–325.

[11] Geng, J., Zhao, Z. (2013). Analysis of amplitude-frequency response on steel wire rope shock absorber (钢丝绳减振器幅频特性研究). *Journal of Taiyuan University of Science and Technology*, 34(3), 233–237.

[12] He, X. (2020). Research progress and developmental recommendations on precision spraying technology and equipment in China (中国精准施药技术和装备研究现状及发展建议). *Smart Agriculture*, 2(1), 133–146.

[13] He, X. (2022). Research and development of efficient plant protection equipment and precision spraying technology in China: a review (高效植保机械与精准施药技术进展). *Journal of Plant Protection*, 49(1), 389–397.

[14] Jeon, H.Y., Womac, A.R., Gunn, J. (2004). Sprayer boom dynamic effects on application uniformity. *Transactions of the American Society of Agricultural Engineers*, 47(3), 647–658.

[15] Langenakens, J., Clijman, L., Ramon, H., Baerdemaeker, J.D. (1999). The effects of vertical sprayer boom movements on the uniformity of spray distribution. *Journal of Agricultural Engineering Research,* 74(3), 281–291.

[16] O'Sullivan, J.A. (1986). Simulation of the behavior of a spray boom with an active and passive pendulum suspension. *Journal of Agricultural Engineering Research*, 35(3), 157–173.

[17] O'Sullivan, J.A. (1988). Verification of passive and active versions of a mathematical model of a pendulum spray boom suspension. *Journal of Agricultural Engineering Research*, 40(2), 89–101.

[18] Qiu, B., Yan, R., Ma, J., Guan, X., Ou, M. (2015). Research progress analysis of variable rate sprayer technology (变量喷雾技术研究进展分析). *Transactions of the Chinese Society of Agricultural Machinery*, 46(3), 59–72.

[19] Ramon, H., Baerdemaeker, J.D. (1997). Spray boom motions and spray distribution: Part I-Derivation of a mathematical relation. *Journal of Agricultural Engineering Research*, 66(1), 23–29.

[20] Tahmasebi, M., Rahman, R.A., Mailah, M., Gohari, M. (2013). Active force control applied to spray boom structure. *Applied Mechanical Material*, 315, 616–620.

[21] Wu, J., Miao, Y. (2012). Dynamic characteristic analysis of boom for wide sprayer with different exciting sources (不同激励源下宽幅喷雾机喷杆的动态特性分析). *Transactions of the Chinese Society of Agricultural Engineering*, 28(4), 39–44.

[22] Xue, T., Li, W., Du, W., Mao, E. Wen, H. (2018). Adaptive fuzzy sliding mode control of spray boom active suspension for large high clearance sprayer (大型高地隙喷雾机喷杆主动悬架自适应模糊滑模控制). *Transactions of the Chinese Society of Agricultural Engineering,* 34(21), 47–56.

[23] Yan, J., Xue, X., Cui, L., Ding, S., Gu, W., et al. (2021). Analysis of dynamic behavior of spray boom under step excitation. *Applied Science*, 11(21), 10129.

[24] Zhuang, T. (2020). *Theoretical analysis and experimental research on boom vibration of large-scale high clearance sprayer* (大型高地隙喷雾机喷杆振动理论分析与试验研究) [Doctoral dissertation, Chinese Academy of Agricultural Mechanization Sciences].

[25] Zhang, X. (2021). *Design and research of spraying rod suspension device for sprayer* (喷杆式喷雾机喷杆悬挂架装置设计与研究) [Master dissertation, Shihezi University].